Physical link of the polar field build-up with the Waldmeier effect broadens the scope of early solar cycle prediction: Cycle 25 is likely to be stronger than Cycle 24

Pawan Kumar, Akash Biswas, Bidya Binay Karak[*]
Department of Physics, Indian Institute of Technology (Banaras Hindu University), Varanasi 221005, India

23 March 2022

ABSTRACT

Prediction of the solar cycle is challenging but essential because it drives space weather. Several predictions with varying amplitudes of the ongoing Cycle 25 have been made. We show that an aspect of the Waldmeier effect, i.e., a strong positive correlation between the rise rate and the amplitude of the cycle, has a physical link with the build-up of the previous cycle's polar field after its reversal. We find that the rise rate of the polar field is highly correlated with the rise rate and the amplitude of the next solar cycle. Thus, the prediction of the amplitude of the solar cycle can be made just a few years after the reversal of the previous cycle's polar field, thereby extending the scope of the solar cycle prediction to much earlier than the usual time. Our prediction of Cycle 25 based on the rise rate of the previous polar field is 137 ± 23, which is quite close to the prediction 138 ± 26 based on the WE2 computed from the available 2 years sunspot data of the ongoing cycle.

Key words: Solar Cycle 25 – Solar Cycle prediction – Waldmeier effect – Polar precursor method – Polar field rise rate

1 INTRODUCTION

The dynamic solar magnetic field is responsible for producing energetic events like solar flares and coronal mass ejections. These events drive space weather which sometimes has hazardous impacts on our space-based society. In a strong cycle, we observe more such events and thus large impacts on the space weather. Hence, predicting the solar cycle strength is of our utmost importance.

As the solar cycle is irregular, the prediction is challenging. Several methods have been applied to predict the amplitudes of the past few cycles and it is not an exception for the Cycle 25 (Petrovay 2020; Nandy 2021). Out of these methods, precursor, in which the information of the previous cycle is used to predict the strength of the cycle, is the most widely used method; see Hathaway et al. (2002); Cameron & Schüssler (2007); Kane (2010); Hazra et al. (2015) and Section 2 of Petrovay (2020).

One important feature of the solar cycle is the Waldmeier effect (Waldmeier 1935), which says that strong cycles take less time to rise, and vice versa. While this correlation is somewhat poor and even difficult to establish (Dikpati et al. 2008; Karak & Choudhuri 2011, hereafter KC11), there exists a robust correlation between the rise rate (slope) and the amplitude of the cycle (Cameron & Schüssler 2008). This correlation exists strongly in all the observed proxies of the solar cycle. KC11 called these two correlations, i.e., the correlations between the rise time and the rise rate of the cycle with the amplitude as WE1 and WE2, respectively. We mention that the Waldmeier effect is not even limited to our sun only, some other sun-like stars do show this feature (Garg et al. 2019).

As the rise rate can be computed when the solar cycle has just

passed the minimum by a few years, we can apply WE2 to predict the amplitude of the solar cycle when the cycle is still growing and has not reached its peak. The current Cycle 25 has passed about 2 years and thus we can predict the amplitude of Cycle 25. This is one of the motivations of the present Letter.

While WE2 is derived based on the observed correlation, there is a strong physical basis for this. KC11 showed that WE2 was robustly reproduced in the Babcock–Leighton type flux transport dynamo models with stochastic fluctuations in the poloidal source. Observations, as well as the dynamo models, suggest that if the polar field at the solar minimum is strong, then the amplitude of the next cycle will be strong (Makarov et al. 1989; Jiang et al. 2007; Wang & Sheeley 2009; Kitchatinov & Olemskoy 2011; Muñoz-Jaramillo et al. 2013; Priyal et al. 2014; Karak & Miesch 2017; Karak et al. 2018; Kumar et al. 2021b). On the other hand, if a cycle is strong, then it rises fast (WE2). Hence, there is a link between the polar field at the solar minimum and the rise rate of the next cycle. We shall explicitly demonstrate this link in the present study.

The most interesting feature that we have found is that the rise rate of the polar field build-up (after its reversal) also determines the rise rate of the next sunspot cycle and thus the amplitude of the cycle. Hence, we do not even need to wait for the time of the solar cycle minimum or the time of the peak of the polar field (which is the usual time for the prediction; Schatten et al. 1978; Choudhuri et al. 2007) to get an idea of the next cycle strength, the rate at which the polar field develops carry this information. In this Letter, we shall present this link both from the observed and the dynamo model data and discuss the physical reason based on the Babcock–Leighton dynamo. Finally, we shall predict the amplitude of the ongoing solar Cycle 25, separately using the rise rate of the current solar cycle and the rise rate of the previous cycle's polar field. We shall show that the

prediction made from these two methods are very close to each other because the physics behind these two are linked.

2 DATA AND METHODS

For our analysis, we have used the monthly sunspot number (SSN) and sunspot area (SSA) data. The SSA data however are not available for Cycle 25. For the observational measures of solar polar field, we have included the polar field strength data (monthly binned) collected from Wilcox Solar Observatory (WSO). To remove the high fluctuations in the data of SSA and SSN, we have used Gaussian smoothing filter with FWHM = 13 and 7 months, respectively (Hathaway et al. 2002). As the current solar cycle 25 has only undergone 2 years from its minimum, we can calculate the rise rates based on this two years data. Hence, to make it uniform for all 13 cycles (Cycle:12–24), we have computed the rise rate for first 2 years of their rise phase only. As the data are not very smooth, and there is some overlap between two consecutive cycles during the first few months of a cycle (Cameron & Schüssler 2008), we excluded the first six month's data from our analysis to avoid any contamination in rise rates due to these reasons. Further, as the rise rate of a cycle is dynamic throughout its evolution, we computed the rise rates at different phases with different time intervals (like 6 to 18 months, 12 to 24 months, etc) and finally we average these values to get one rise rate for each cycle. For computing the rise rate of the polar field, we compute it within the first three years after the reversal, as there is no overlap between two consecutive cycles in the polar field data. Again here also we compute the rates at different intervals and average those to get one rise rate for a cycle.

3 RESULTS AND DISCUSSION

3.1 WE2 and the prediction of Cycle 25

Figure 1 shows the scatter plots of the rise rates with the amplitudes of the SSN (a) and SSA (b). We find a strong correlation between these two quantities for both the data with linear (Pearson) correlation coefficients of 0.87 for SSN and 0.89 for SSA data. These results reproduce WE2 (Waldmeier 1935; Karak & Choudhuri 2011). The straight lines in Figure 1 are obtained from the linear regression based on Bayesian probabilistic approach (using Python's Pymc3 routine); see figure caption for the fitted parameters. The strong correlation between these quantities in Figure 1 implies that if the rise rate of a cycle is known even for some part of its rising phase, then the amplitude of the cycle can be predicted well in advance. To test the reliability of this prediction method, we predict the amplitudes of the last few observed cycles and compare them with observed values. We note that when we predict the amplitude of a given cycle, we exclude the data for that cycle while computing the regression relation. In Table 1, we mention our predicted peak values along with their errors for previous 6 cycles (Cycle: 19–24) and the actual observed values. We can see that the the predicted values are not too far from the actual ones. For some cycles, like Cycle 22, the predicted value is quite different from the observed ones, but considering the error in the regression, it is not too much off from the allowed range. We do the same exercise using SSA data and the predicted amplitude of SSA are given in Table 1. However, in this case, we see a somewhat larger deviation in predicted values from the actual observations, although the correlation between the rise rate and the observed amplitude is better than that in the SSN data. To compare these predicted peak areas with the observed SSN, we convert the
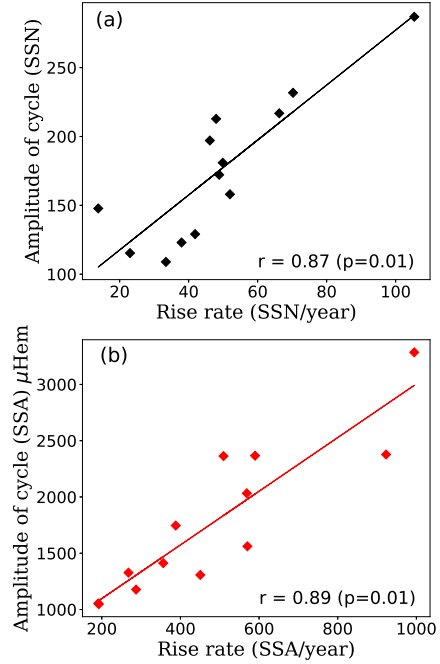

Figure 1. Scatter plots between the rise rates and the amplitudes of the cycles for SSN (a) and SSA (b). Lines are the linear regressions: $y = mx + c$, where $m = 2.001 \pm 0.308$ and $c = 77.305 \pm 16.545$ for SSN and $m = 2.423 \pm 0.114$ and $c = 596.789 \pm 62.028$ for SSA.

Table 1. Predictions of the solar cycle *amplitudes* using the rise rates of SSN and SSA (in μHem) for the last few known cycles and the ongoing Cycle 25.

Cyc. No	Obs. SSN	Predicted peak SSN	Obs. SSA	Predicted SSA	SSN from Col. 5
25	– – –	138 ± 26	– – –	– – –	– – –
24	116	125 ± 26	1054.0	1058.2 ± 84.6	121 ± 17
23	181	177 ± 33	1746.1	1536.3 ± 83.1	157 ± 17
22	213	170 ± 30	2354.5	2026.2 ± 129.3	195 ± 20
21	232	216 ± 40	2363.1	1831.5 ± 122.3	180 ± 19
20	158	183 ± 32	1561.4	1978.8 ± 128.8	191 ± 20
19	287	290 ± 72	3285.2	3008.6 ± 177.2	270 ± 24

predicted SSA into the SSN by employing the regression relation between SSN and SSA, which are listed in the last column of Table 1. Overall, prediction based on the rise rate of both sunspot number and area supports our idea.

Finally we predict the peak of the ongoing Cycle 25 based on its available SSN data. We find the predicted amplitude of Cycle 25 to be 138 ± 26; see Table 1. As we do not have SSA data for this cycle, we cannot predict the peak of SSA for Cycle 25 directly from the rise rate of SSA data.

WE2 relation also gives how much time the cycle will take to reach its peak from its minimum. For Cycle 25, this value comes to be 4.5 ± 0.8 years, which is quite close to the average time of 4.58 ± 0.81 years between the cycle minimum to maximum as reported in Kumar et al. (2021a, see their Table 1). Therefore, we predict that the Cycle 25 will attain peak at 2024.5 ± 0.8. For better visualization, our predicted peak SSNs with their error ranges are shown in Figure 2.
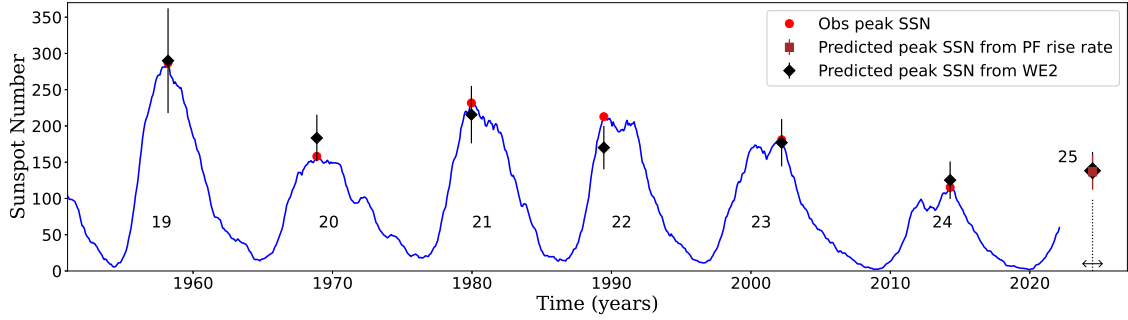
Figure 2. Comparison of our prediction with observations. Temporal variation of the observed SSN is shown by the blue curve with red dots showing the observed peaks. The predicted amplitudes are shown by black squares and their errors by vertical lines. The time of the peak of the predicted Cycle 25 is shown by the vertical dotted line with the error by a horizontal arrow. The prediction for Cycle 25 using *the rise rate* of the previous cycle's polar field is shown by a (dark red) square.
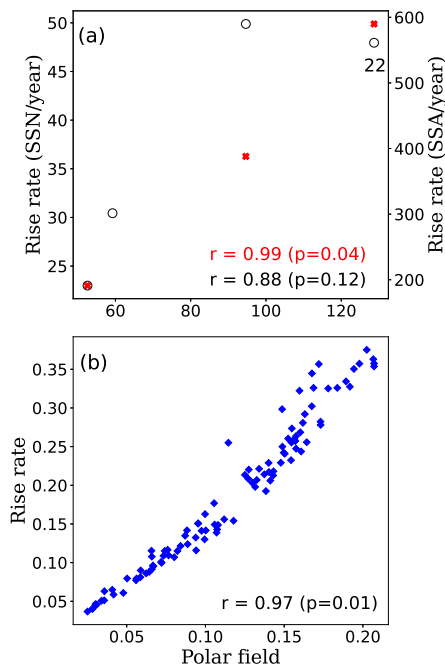

Figure 3. Scatter plots between the polar field at solar cycle minimum and the rise rate of next cycle. (a) The open circles and the red crosses represent the rise rates calculated from SSN and SSA, respectively. (b) Same as (a) but from a dynamo model.

3.2 Connecting WE2 with the previous cycle polar field

We would like to mention that although our prediction in §3.1 is based on an empirical relation which holds 'statistically' and hence the prediction for certain cycles (like cycle 22) may not perfectly agree with the observation. However, we still make prediction because our method is based on a strong physical ground. It was shown that WE2 relation (on which our prediction is based) is a robust feature of solar dynamo (Karak & Choudhuri 2011; Pipin & Kosovichev 2011; Pipin & Sokoloff 2011). Particularly, KC11 found a strong correlation for WE2 in all the simulations they have performed. They explained that fluctuations in the generation of poloidal field (Babcock–Leighton process), makes the polar field at the solar minimum unequal for different cycles. As the polar field gives rise to

the toroidal field and the sunspot for the next cycle, strong polar field makes the next cycle strong. This is also established in the observational data (Makarov et al. 1989; Choudhuri et al. 2007; Jiang et al. 2007; Wang & Sheeley 2009; Kitchatinov & Olemskoy 2011; Muñoz-Jaramillo et al. 2013; Priyal et al. 2014). Finally if the cycle is strong, it has to rise fast.

Based on above discussion, we expect that the rise rate of a cycle should be directly linked with the poloidal field at the previous minimum. To check this link, we compute the linear correlation between these two, based on the observed polar field data for last four cycles; see Figure 3(a). We observe a reasonably good correlation between these two quantities from SSN and SSA data. However, the data of SSN for Cycle 22 is showing some deviation from the linear trend. This may be due to the fact that we are calculating the rise rate based on only first two years data (to make it consistent with the available data for Cycle 25). Furthermore, the polar field data are imperfect due to limited observations in the polar regions (Bertello et al. 2014; Mordvinov et al. 2022). Hence, the reliability of this relation cannot be endorsed with limited data.

Therefore, we try to explore this link between the polar field and the rise rate of the next cycle using Babcock–Leighton type dynamo theory. To do so, we have taken the data from the dynamo model: Run 2DR2 as presented in (Kumar et al. 2021a) which is produced using *Surya* code (Chatterjee et al. 2004). We compute the correlation between the polar field at a cycle minimum and the rise rate of the following cycle from the data of 100 cycles in the same manner as done for the observed data. We find a high correlation as seen in Figure 3(b). This supports the fact that a strong poloidal field indeed makes the following cycle rise faster and hence the cycle becomes stronger, obeying WE2. So, we believe that our prediction for the ongoing cycle 25 should be comparable with the prediction made by other groups using the observed polar field data but not the same because there is one more physical process involved in it that we shall discuss in §3.3. To facilitate the comparison, we enlist our predicted values of the amplitude and time of the peak for cycle 25 with various other groups in Table 2. We find that our value is slightly larger than most of the predictions, but not too much considering the error range.

3.3 Correlation with the rise rate of the polar field and the prediction of Cycle 25

Finally, further going one step backwards in the evolution of solar cycles, we find a very interesting relation that the rise rate of the polar field build-up (after reversal) has a correlation with the amplitude of

Table 2. Comparison of our predictions for Solar Cycle 25 (P1: using the rise rate of the SSN, P2: using the rise rate of the previous cycle's polar field) with predictions by other groups who used observed polar precursor.

Authors	Predicted SSN	Time
This work: P1	138 ± 26	2024.5 ± 0.8
: P2	137 ± 23	
Kumar et al. (2021a)	120 ± 25	– – –
Hazra & Choudhuri (2019)	140.5 ± 2.5	– – –
Pesnell & Schatten (2018)	135 ± 25	2025.2 ± 1.5
Petrovay et al. (2018)	130	Late 2024
Gopalswamy et al. (2018)	148	– – –
Bhowmik & Nandy (2018)	118	2024 ± 1
Upton & Hathaway (2018)	110	– – –

the next cycle; see Figure 4(a). We note that here we have used the hemispheric data for the correlation. We find a similar strong correlation ($r = 0.99$, $p = 0.01$) for both SSN and SSA data. We note that we had computed the average rise rate during the first three years after the polar field reversal. If we go beyond 3 years, then the polar field tends to saturate and the rise rate poorly correlates with the amplitude of the next cycle. Unfortunately, again the reliability of this relation cannot be proven based on only three data points. However, we find a strong relation between these two quantities in the dynamo model (again from Run 2DR2); see Figure 4(b). As this relation holds good, we obviously expect a strong correlation between the rise rate of the polar field build-up and the rise rate of the next cycle, which is indeed seen in Figure 4(c).

The physics behind this correlation is not difficult to understand. In the Babcock–Leighton process, the decay and dispersal of tilted BMRs produces polar field in the Sun. When a sunspot cycle reaches its maximum, the polar field is usually reversed and then as the new BMRs emerge, the polar field increases (due to continuous supply of the trailing polarity flux from low latitudes) while the sunspot cycle decline. Hence, if the polar field in a cycle rises rapidly, then the toroidal field for the next cycle will also be amplified rapidly. This causes the next sunspot cycle to rise fast and also makes it strong.

One follow-up question is why the rise rate of the polar field build-up is not the same for all cycles. It is because the generation of poloidal field involves some randomness, particularly due to scatter in the BMR tilts (Jiang et al. 2014; Hazra et al. 2017; Karak & Miesch 2017; Jha et al. 2020) and the latitudinal positions of BMRs (Karak 2020). In fact, there is indication that the decline phase of the cycle (during which the polar field is built up after reversal) is more irregular having many anti-hale and non-Joy BMRs (Zhukova et al. 2022; Mordvinov et al. 2022), that can disturb the growth of the polar field considerably. Due to this inherent randomness in the Babcock–Leighton process, even if two cycles decay identically, their corresponding polar field can build up differently.

In conclusion, if the correlation between the rise rate and the amplitude of the next cycle, as seen in the observed data (Figure 4(a)) and in the dynamo model (Figure 4(b)) really holds good in the Sun, then we can make prediction of the solar cycle a few years before the time of the previous polar field peak or the solar minimum. This considerably increases the scope of the predictability of the solar cycle. Using the observed regression relation between the polar field rise rate and the amplitude of the next solar cycle (Figure 4(a)), we find the peak of the ongoing Cycle 25 to be 137 ± 23. Instead of hemispheric SSN data, if we use SSA data, and then convert the predicted value into SSN (using the regression relation between the SSN and SSA), we get the peak value to be 144 ± 3. So we clearly see that these two values are quite close to the one that we have obtained using WE2 relation (138 ± 26) in §3.1.
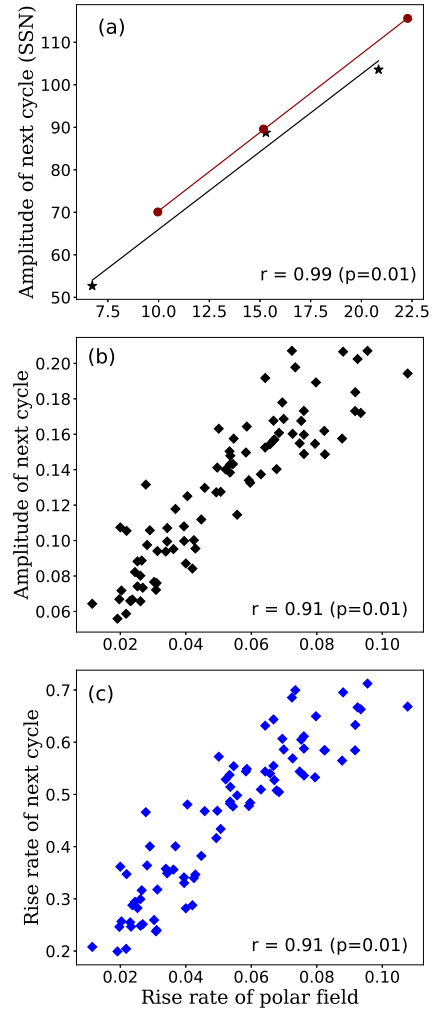

Figure 4. (a) Scatter plot between rise rate of observed polar field and the amplitude of the next cycle SSN. Regression lines: $y = mx + c$, where m = 3.677 ± 0.876 and c = 29.093 ± 13.517 for the northern (asterisks) and m = 3.689 ± 0.912 and c = 33.405 ± 15.311 for southern hemispheres (filled circles). (b) Same as (a) but from the dynamo model. (c) Same as (b) but for the rise rate of the next sunspot cycle.

4 CONCLUSIONS

We have utilised a robust feature of Waldmeier effect namely, the rise rate of a cycle is strongly correlated with its amplitude (WE2) and we have shown that a reliable prediction of a solar cycle can be made when the cycle has just past a few years from its minimum. The ongoing solar cycle has passed about two years, and using this data, we predict that the amplitude of Cycle 25 will be 138 ± 26 and it will attain peak around mid to late 2024. Hence, the ongoing cycle will be slightly stronger than the previous Cycle 24. Our predicted strength is also significantly larger than the NOAA/NASA Prediction Panel [1], which predicted the peak SSN of Cycle 25 to be 115 ± 10.

We have shown that this prediction method (WE2) is based on a strong physical ground. If a polar field of a cycle is strong, then the next cycle has to be strong and it will also rise fast. Hence, our prediction based on the rise rate should be comparable to the one

---

[1] https://www.swpc.noaa.gov/news/solar-cycle-25-forecast-update

based on the polar field of the previous cycle; see Table 2. But this is not the complete story. If the polar field builds up (after its reversal) rapidly, then the next cycle will be strong and vice versa. Therefore, we find a strong correlation between the rise rate of the polar field and the amplitude of the next cycle, both in observations and in dynamo models (also see Appendix of Kumar et al. 2021a). Based on the observed regression relation between the rise rate of the previous cycle's polar field build-up with the amplitude of the sunspot cycle, we predict the amplitude of the ongoing Cycle 25 to be 137 ± 23.

Hence, our predictions made from both methods, namely using the rise rate of sunspot cycle and the rise rate of the previous cycle's polar field, match quite well. This agreement is because of the fact that they are linked. The polar field of the previous cycle gives rise to the toroidal field and the sunspot of the current cycle and thus, how rapidly the Sun builds up its polar field determines the rise rate of the next cycle. This link between the rate of build-up of the polar field with the amplitude of the next cycle suggest that we can predict the amplitude of the next solar cycle just after about 2-3 years of the reversal of its polar field (or up to about 9 years before the peak of a cycle). Earlier Kumar et al. (2021a) have shown that the prediction of the cycle can be made just after 4 years of the reversal of the polar field. Hence, this study, along with our present work, extends the scope of solar cycle prediction by a considerable amount of time.

ACKNOWLEDGEMENTS

DATA AVAILABILITY

We have used the SSN data available at SILSO[2] and SSA from the Royal Greenwich Observatory (RGO)[3]. The hemispheric SSN data has been collected from Veronig et al. (2021)[4]. Polar field data is taken from Wilcox Solar Observatory (WSO)[5]. Data from our dynamo models and the analyses codes can be shared upon a reasonable request.

REFERENCES

Bertello L., Pevtsov A. A., Petrie G. J. D., Keys D., 2014, Sol. Phys., 289, 2419
Bhowmik P., Nandy D., 2018, Nature Communications, 9, 5209
Cameron R., Schüssler M., 2007, ApJ, 659, 801
Cameron R., Schüssler M., 2008, ApJ, 685, 1291
Chatterjee P., Nandy D., Choudhuri A. R., 2004, A&A, 427, 1019
Choudhuri A. R., Chatterjee P., Jiang J., 2007, Physical Review Letters, 98, 131103
Dikpati M., Gilman P. A., de Toma G., 2008, ApJ, 673, L99
Garg S., Karak B. B., Egeland R., Soon W., Baliunas S., 2019, arXiv e-prints, p. arXiv:1909.12148
Gopalswamy N., Mäkelä P., Yashiro S., Akiyama S., 2018, Journal of Atmospheric and Solar-Terrestrial Physics, 176, 26
Hathaway D. H., Wilson R. M., Reichmann E. J., 2002, Sol. Phys., 211, 357
Hazra G., Choudhuri A. R., 2019, ApJ, 880, 113
Hazra G., Karak B. B., Banerjee D., Choudhuri A. R., 2015, Sol. Phys., 290, 1851
Hazra G., Choudhuri A. R., Miesch M. S., 2017, ApJ, 835, 39
Jha B. K., Karak B. B., Mandal S., Banerjee D., 2020, ApJ, 889, L19
Jiang J., Chatterjee P., Choudhuri A. R., 2007, MNRAS, 381, 1527
Jiang J., Cameron R. H., Schüssler M., 2014, ApJ, 791, 5
Kane R. P., 2010, Sol. Phys., 261, 209
Karak B. B., 2020, ApJ, 901, L35
Karak B. B., Choudhuri A. R., 2011, MNRAS, 410, 1503
Karak B. B., Miesch M., 2017, ApJ, 847, 69
Karak B. B., Mandal S., Banerjee D., 2018, ApJ, 866, 17
Kitchatinov L. L., Olemskoy S. V., 2011, Astronomy Letters, 37, 656
Kumar P., Nagy M., Lemerle A., Karak B. B., Petrovay K., 2021a, ApJ, 909, 87
Kumar P., Karak B. B., Vashishth V., 2021b, ApJ, 913, 65
Makarov V. I., Makarova V. V., Sivaraman K. R., 1989, Sol. Phys., 119, 45
Mordvinov A. V., Karak B. B., Banerjee D., Golubeva E. M., Khlystova A. I., Zhukova A. V., Kumar P., 2022, MNRAS, 510, 1331
Muñoz-Jaramillo A., Dasi-Espuig M., Balmaceda L. A., DeLuca E. E., 2013, ApJ, 767, L25
Nandy D., 2021, Sol. Phys., 296, 54
Pesnell W. D., Schatten K. H., 2018, Sol. Phys., 293, 112
Petrovay K., 2020, Living Reviews in Solar Physics, 17, 2
Petrovay K., Nagy M., Gerják T., Juhász L., 2018, Journal of Atmospheric and Solar-Terrestrial Physics, 176, 15
Pipin V. V., Kosovichev A. G., 2011, ApJ, 741, 1
Pipin V. V., Sokoloff D. D., 2011, Phys. Scr., 84, 065903
Priyal M., Banerjee D., Karak B. B., Muñoz-Jaramillo A., Ravindra B., Choudhuri A. R., Singh J., 2014, ApJ, 793, L4
Schatten K. H., Scherrer P. H., Svalgaard L., Wilcox J. M., 1978, Geophys. Res. Lett., 5, 411
Upton L. A., Hathaway D. H., 2018, Geophys. Res. Lett., 45, 8091
Veronig A. M., Jain S., Podladchikova T., Pötzi W., Clette F., 2021, A&A, 652, A56
Waldmeier M., 1935, Astronomische Mitteilungen der Eidgenössischen Sternwarte Zurich, 14, 105
Wang Y.-M., Sheeley N. R., 2009, ApJ, 694, L11
Zhukova A., Khlystova A., Abramenko V., Sokoloff D., 2022, MNRAS,

This paper has been typeset from a TeX/LaTeX file prepared by the author.

---

[2] http://sidc.oma.be/silso/DATA/SN_ms_tot_V2.0.txt
[3] https://solarscience.msfc.nasa.gov/greenwch.shtml
[4] https://wwwbis.sidc.be/silso/extheminum
[5] http://wso.stanford.edu/Polar.html